Asian Journal of Atmospheric Environment
Vol. 3-1, pp.1-8, June 2009
doi: 10.5572/ajae.2009.3.1.001

Enhancement of Aerosol Concentration in Korea due to the Northeast Asian Forest Fire in May 2003

Hee-Jin In, Yong Pyo Kim[1),*] and Kwon H. Lee[2)]

Forecast Bureau, Korea Meteorological Administration, Seoul 156-720, Korea
[1)]Department of Environmental Science and Engineering, Ewha Womans University, Seoul 120-750, Korea
[2)]Earth System Science Interdisciplinary Center (ESSIC), University of Maryland, College Park, MD 20742, USA

*Corresponding author. Tel: +82-2-3277-2832, E-mail: yong@ewha.ac.kr

ABSTRACT

Enhancement of aerosol optical thickness (AOT) and surface aerosol mass concentration in Korea for an active forest fire episode in Northeast Asia were estimated by Community Multi-scale Air Quality (CMAQ) model. MODIS/TERRA remote detects of fires in Northeast Asia for May 2003 gave a constraint for estimation of wildfire emissions with an NDVI distribution for recent five years. The simulated wildfire plumes and enhancement of AOT were evaluated and well resolved by comparing multiple satellite observations such as MODIS, TOMS, and others. Scatter plots of observed daily mean aerosol extinction coefficient versus PM_{10} concentration in ground level in Korea showed distinctively different trends based on the ambient relative humidity.

Key words: Asian forest fire, Aerosol optical thickness, CMAQ model, PM_{10} in Korea, Satellite fire product

1. INTRODUCTION

The regional atmosphere of northeast Asia is influenced by frequent soil dust emission and biomass burning in spring. The origins and transport characteristics of Asian dust have been studied numerically (see, for example, In and Park, 2002). However, biomass burning and wild-fire have not been much investigated with three dimensional modeling approaches. Biomass burning is a significant global source of trace gas and aerosols which affect on climate environment system (Levine *et al*., 1995). In addition to the tropics, fires in the boreal forests are also major global source for ambient trace species including ambient particles.

Large-scale fire occurrences have been successfully monitored by satellites such as Advanced Very High Resolution Radiometer (AVHRR) on board the polar orbiter NOAA satellites, Geostationary Orbiting Environmental Satellite (GOES), and the Along Track Scanning Radiometer (ATSR) (Arino and Rosaz, 1999). The Moderate Resolution Imaging Spectroradiometer (MODIS) (Kaufman *et al*., 1998) substantially improved capabilities for fire mapping as compared with the AVHRR and its swath provides unique opportunity to analyze the fine-scale active fires.

In May 2003, a large number of fires were detected along the Russian borders with Mongolia and China between 45 and 60 N with the most intense fire in the regions near Lake Baikal. The contribution from the fires to the ambient air quality in Korea (Lee *et al*., 2005) and in western North America (Jaffe *et al*., 2004) was observed. Damoah *et al*. (2004) demonstrated transport of forest fire smoke for 17 days using a Lagrangian particle dispersion model. They validated their model result by using the observations from the multiple platforms of satellite measurements. But their results had limitations to elucidate the contribution of particles to aerosol optical thickness (AOT) and to quantify ground level aerosol concentration because the model did not include chemical reactions. Jaffe *et al*. (2004) reported the relationship between the annual Russian area burned and the background O_3 and CO concentrations in western North America. However, aerosol chemistry was not included in their model simulation.

In this study, the variations of aerosol mass concentration and AOT which is a good indicator for accounting radiative properties in the climate simulation are estimated by Community Multi-scale Air Quality (CMAQ) model with a constraint of satellite fire detection for an active Northeast Asian fire event of May 2003. We first examine fire products of remote sensing in simulating fire effects on atmospheric environment by comparing model results with the MODIS retrieved AOTs and satellite observations and observed surface aerosol mass concentrations. Then, the variables that affect the surface aerosol concentration are discussed.

2. MODELING

CMAQ version 4.3 (Byun and Shere, 2006; Byun *et al*., 2003; Byun and Ching, 1999) and Penn State-NCAR fifth generation mesoscale model (MM5) (Grell *et al*. 1994), which provides meteorological fields, were used for the simulation. Both of them were configured with a single domain using a 81×81 km horizontal grid spacing which covered the northeast Asia region, including northern part of Russia, China, Korea and Japan as shown in Fig. 1. In the vertical, 23 un-

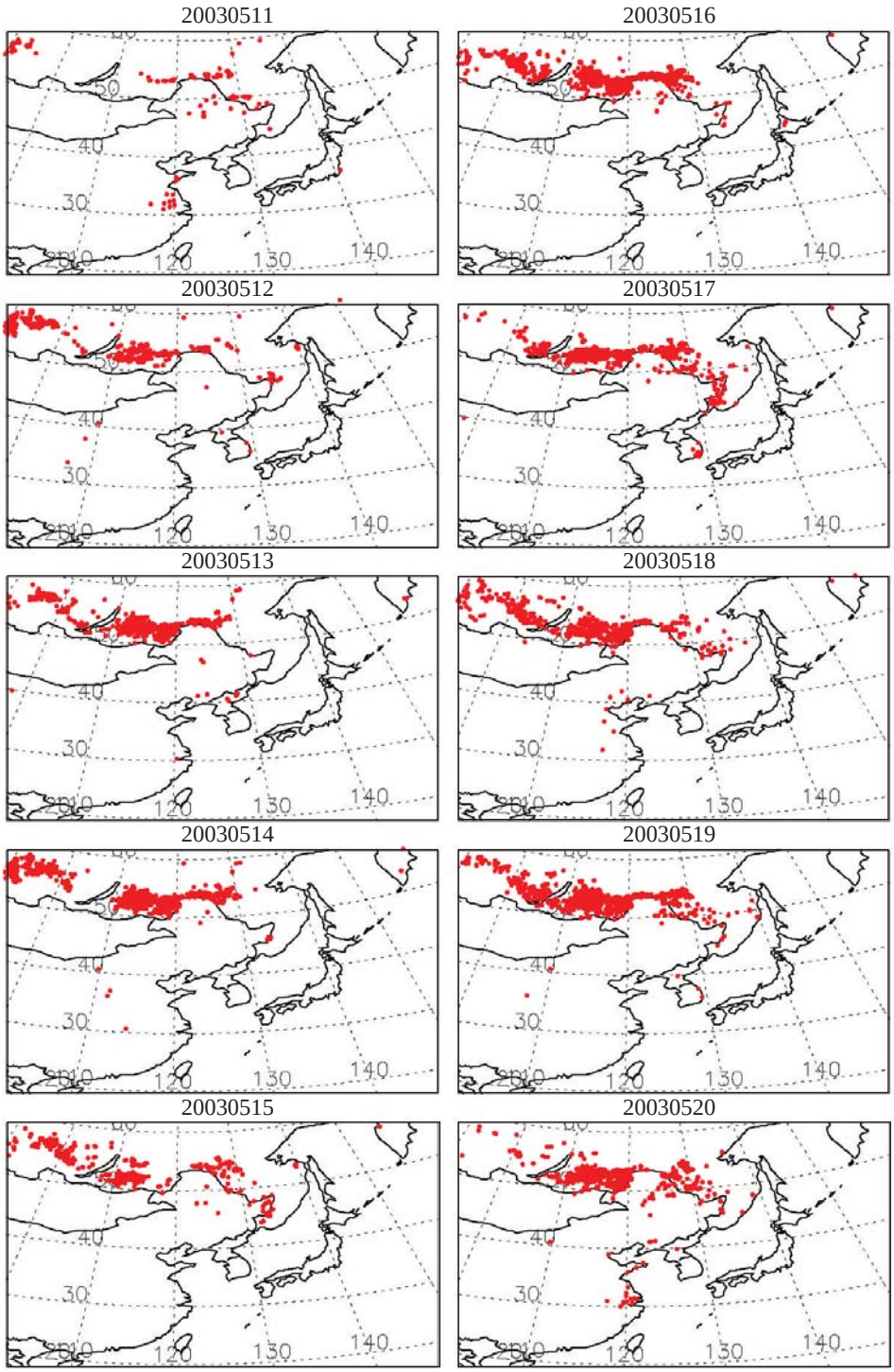

Fig. 1. Locations of the hot spots which are detected by MODIS satellite in Northeast Asia for the middle of May 2003.

evenly spaced terrain-following sigma levels were employed with grid spacing stretching from approximately 30 m above surface to 4,000 m at the model top near 14 km (100 mb). The MM5 was assimilated every six hourly using the National Centers for Environmental Prediction (NCEP)'s NCAR reanalysis.

The emission inventory compiled by Streets *et al*. (2003), which was evaluated for TRACE-P campaign modeling studies, was used to provide anthropogenic gaseous and primary aerosol sources for simulation in this study. For the emissions of CO and $PM_{2.5}$, the emission factors of Andreae and Merlet (2001) were used to convert biomass burnt to emission amounts. The estimate of burned biomass can be expressed by an equation; Biomass burned (M_{BB})=A × B × C (Seiler and Crutzen, 1980). M_{BB} is the amount of biomass burnt, A is the area burnt (m^2), B is the biomass density (g m^{-2}), and C is the burning efficiency (g g^{-1}), where biomass density and burning efficiency are given as dependent on the class of vegetation.

For the estimation of burned area, we allocated a fire pixel detected by MODIS/TERRA satellite (Fig. 1), which had a 1 × 1 km resolution, into modeling grids with 1 km^2 area and then all the pixels were considered as totally burned independently of the number of times they were flagged as burned during a one month period. Biomass density was estimated based on the values found in the literature (Barbosa *et al*., 1999) and on the accumulated normalized difference vegetation index (NDVI) which was observed by satellites and provided weekly by the EROS Data Center, U.S. Geological Survey. NDVI mappings were composited weekly and have a 1.1 km (0.6 mile) spatial resolution. Burning efficiency was assessed with a dryness index that was based on the relative greenness index (RGI) which was also derived from the NDVI. The accumulated NDVI was computed for every year on a pixel by pixel basis, by summing the consecutive weekly NDVI values between the minimum and the maximum found. The accumulated NDVI was then used to estimate the biomass density for a given year in each pixel.

According to In *et al*. (2007), CMAQ overestimated ground level carbonaceous aerosol concentrations when wildfire emissions were allocated up to mixed layer height. Thus, biomass burning emission was distributed with the assumption of vertical well mixing from ground level up to 5 km height in model layer based on the vertical evolution of CO mixing ratio which was observed by the Measurement Of Pollution In The Troposphere (MOPITT) on board TERRA satellite, because CO and biomass mass burning are well correlated in wildfire emission region.

The mass reconstruction technique (Pitchford and Malm, 1994) in CMAQ aerosol module was used to calculate aerosol extinction coefficient (β_{ext}). The aerosol extincetion coefficient is defined as β_{ext} [km^{-1}]= β_{sp}+0.01 [km^{-1}], where β_{sp} is the aerosol extinction coefficient that must be adjusted by 0.01 [km^{-1}]. AOT is defined as the vertical sum of the aerosol extinction coefficient of each layer and β_{sp} is estimates as follows:

$$\beta_{sp}\,[km^{-1}] = 0.003 \times f(RH) \times \{[\text{ammonium sulfate}] + [\text{ammonium nitrate}]\} + 0.004 \times [\text{organic mass}] + 0.01 \times [\text{Light Absorbing Carbon}] + 0.001 \times [\text{fine soil}] + 0.0006 \times [\text{coarse mass}]$$

3. RESULTS AND DISCUSSION

3.1 Comparison of CMAQ AOT with the Satellite Measurements

The AOTs from MODIS remote observations are retrieved using the algorithm by Lee *et al*. (2005) with a 1 × 1 km spatial coverage and mapped to CMAQ grid cells by searching a nearest-neighbor through all pixels on every day for one month simulation period. Fig. 2 shows the comparison of the satellite observation and CMAQ simulations for selected episode (May 7-May 10), demonstrating the transport of aerosols originating from biomass burning. On May 7, CMAQ derived AOT distribution is elevated over high Siberian areas where intense hot spots were detected as shown in Fig. 1.

MODIS AOTs were not complete in covering the whole modeling domain. Thus, we additionally use the observed Total Ozone Mapping Spectrometer (TOMS) aerosol index (AI), which has global coverage though its resolution is coarse (2.5 by 2.0 deg) to validate the CMAQ simulation results. For example, existence of aerosol band extending eastward on 50 N latitude is justified by comparing the TOMS AI distribution on the day. For the consecutive days, CMAQ derived AOT spatial distribution patterns show that the wildfire emissions from northern latitude as 55-60 N evolved southward about 35 N and gave effects on visual environments in northeast Asia. And the evolutionary characteristics and southeastward spatial extension corresponds very well with the TOMS AI and MODIS AOT distributions.

However, there are some days in which the MODIS AOT results and the CMAQ simulation do not match well. Fig. 3 shows the comparison of the satellite observation and CMAQ simulations for the selected days (May 7, 14, 18, and 20) along with TOMS AI and MOPPIT CO data. On May 7, 14, and 18, two results agree reasonably. However, on May 20, the CMAQ simulation result shows different distribution from the MODIS AOT result.

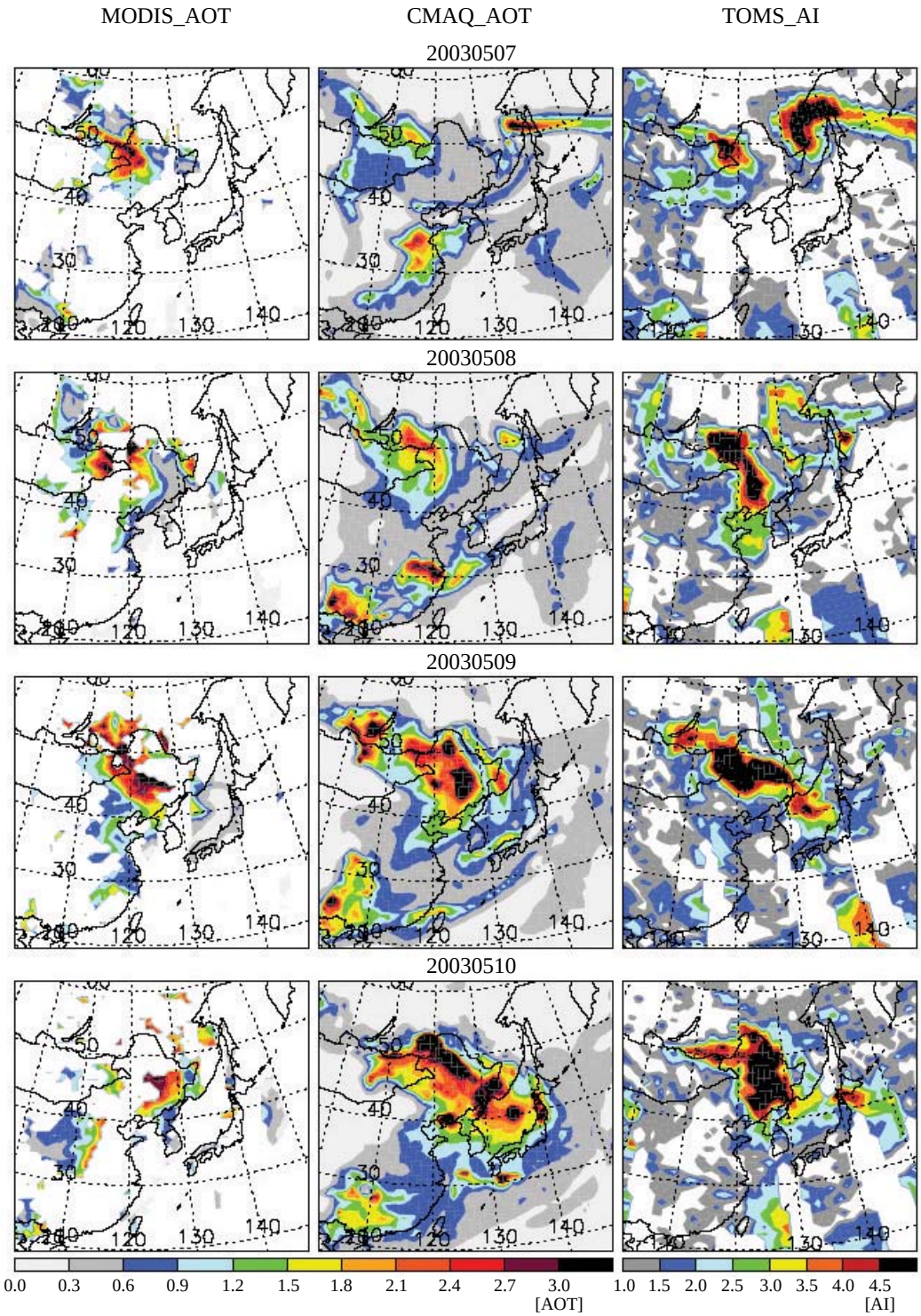

Fig. 2. MODIS retrieved AOT (first column), CMAQ derived AOT (second column), and the observed aerosol index (AI) by TOMS between May 7 and 10, 2003.

3.2 Aerosol Mass Concentration Versus Aerosol Extinction Coefficient

We investigate the dependency of aerosol extinction coefficient on aerosol mass concentration and relative humidity (RH) on ground level because surface aerosol extinction coefficient is a measure of visual range.

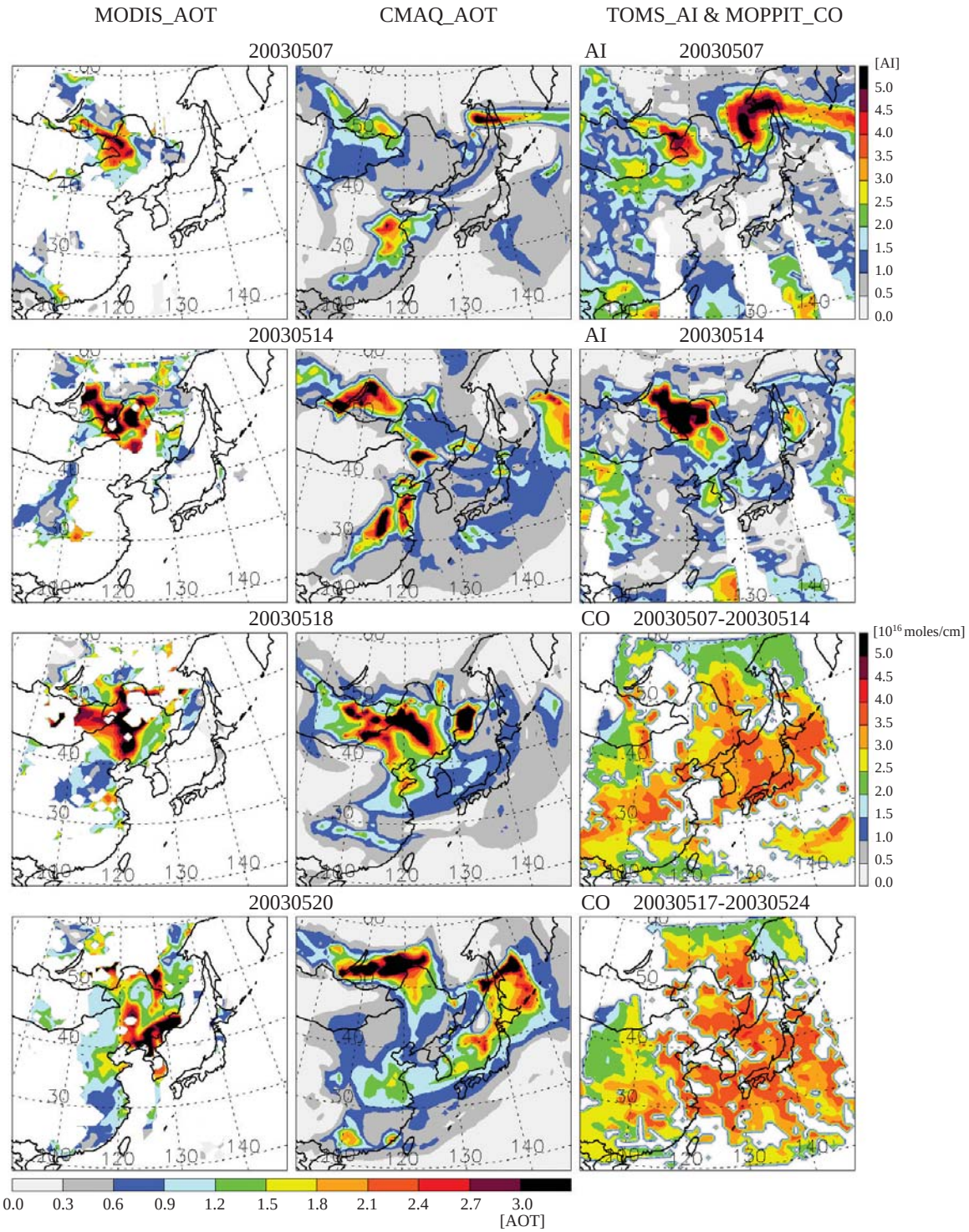

Fig. 3. MODIS retrieved AOT (first column), CMAQ derived AOT (second column), and the observed aerosol index (AI) by TOMS and CO by MOPPIT (third column) in the selected days of May 2003.

Scatter plots of the observed daily mean aerosol extinction coefficient versus PM_{10} concentration in ground level in Korea according to RH (Fig. 4a) show that the relationship (linear regression parameters and correlation coefficient) varied based on the ambient RH. Under moderate humidity condition, ($60\% \leq RH <$

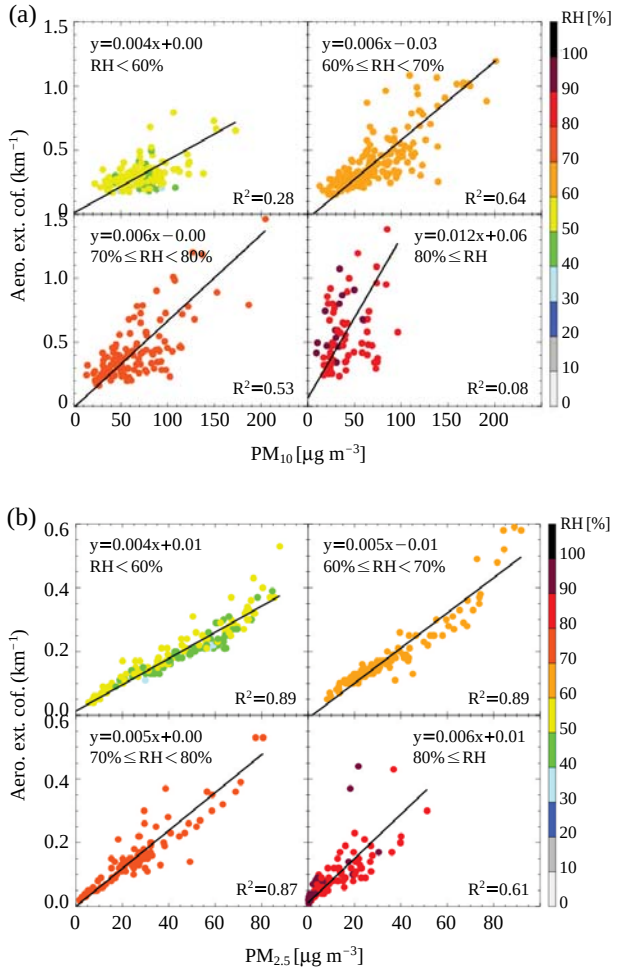

Fig. 4. Scatterplots of (a) the observed daily mean surface PM_{10} concentrations and (b) the simulated surface $PM_{2.5}$ concentrations versus simulated extinction coefficients.

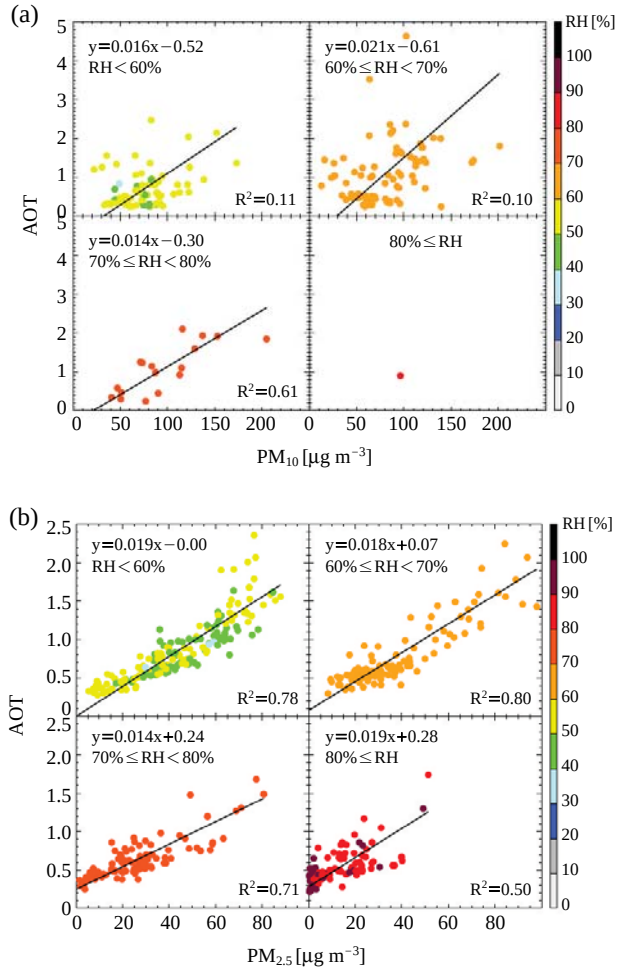

Fig. 5. Scatterplots of (a) the observed daily mean surface PM_{10} concentrations versus MODIS AOT and (b) the simulated surface $PM_{2.5}$ concentrations versus simulated AOTs.

80%) visual ranges were related well with the aerosol mass concentration (R^2=0.64 in 60%≤RH<70% and R^2=0.53 in 70%≤RH<80%). However, at both dry and very humid conditions, the correlation between visual range and aerosol mass concentration became worse (R^2=0.28 in RH≤60% and R^2=0.08 in 80<RH). The slope of the regression lines increased with RH, indicating the contribution of aerosol concentration to visual range grew by the hygroscopic aerosols such as sulfate and nitrate (Malm *et al.*, 1994).

Simulated aerosol extinction coefficient and $PM_{2.5}$ concentration (Fig. 4b) present better linear relationship with higher correlation coefficient of R^2=0.61-0.89, having nominal differences depending on RH. It suggests that fine aerosols were more related with atmospheric visibility and the CMAQ mass reconstruct method to estimate aerosol extinction coefficient does not represent aerosol hygroscopic characteristics well enough. The mass reconstruct method considers aerosols except sulfate and nitrate as non-hygroscopic. However, Malm *et al.* (2005) found that hygroscopicity of organic carbon aerosols which were major component in wild fire burning. Fresh organic carbon aerosols were generally hydrophobic but as aerosols aged during transport to Korea from their origin in Russia, they became hydrophilic and have hygroscopic characteristics. Such discrepancy calls for implements of hygroscopic characteristics of organic carbon aerosols in the CMAQ model.

AOT and ground level aerosol mass concentration are less correlated as shown in Fig. 5a (from MODIS observed AOT and PM_{10}) and 5b (from simulated AOT and $PM_{2.5}$). AOT is a column integrated value without vertical resolution of aerosol properties thus it does

not recognize whether aerosols are in elevated plume that does not affect surface visibility or in the boundary layer. Therefore, the comparison between the surface aerosol mass concentration and the AOT generates worse correlation than the correlation between ground level aerosol extinction coefficient and aerosol mass concentration both in observation and simulation. Regression between AOT and aerosol mass concentration in the simulation also generates slight differences according to relative humidity with correlation coefficients of R^2=0.50-0.80. MODIS observed AOT and the observed PM_{10} concentration show very poor correlation between them.

4. SUMMARY

We simulated $PM_{2.5}$ concentration and AOT using the US EPA's CMAQ model in an active wild land fire season in northeast Asia. For May 2003, a large number of fires were detected along the Russian borders with Mongolia and China between 45 and 60 N with the most intense fire in the regions near Lake Baikal. The estimation of fire emission were constraint by the fire detects by MODIS/TERRA satellite, biomass density, and burning efficiency which were derived from the NDVI data based for five consecutive years by satellite remote sensing.

General spatial pattern of the CMAQ derived AOT showed agreement with several satellite measurements as southeastward evolution of wildfire aerosols from their origins to the northern Pacific. We found that relative humidity was an important parameter to correlate the fine aerosol mass concentration with atmospheric visibility. CMAQ mass reconstruct method to estimate aerosol extinction coefficient did not represent aerosol hygroscopic characteristics enough.

ACKNOWLEDGEMENTS

This work was supported by National Research Laboratory program (No. R0A-2006-000-10221-0) funded by the Korea Science and Engineering Foundation. NASA and KNMI are acknowledged for providing the satellite data used in this study.

REFERENCES

Andreae M.O. and P. Merlet (2001) Emissions of trace gases and aerosols from biomass burning. Global Biogeochemical Cycles, 15(4), 955-966.

Arino O. and J. Rosaz (1999) 1997 and 1998 world ATSR fire atlas using ERS-2 ATSR-2 data, In Proceedings of the Joint Fire Science Conference, Boise, pp. 15-17.

Barbosa P.M., D. Stroppiana, J.-M. Gregoire, and J.M.C. Pereira (1999) An assessment of vegetation fire in Africa (1981-1991): Burned areas, burned biomass, and atmospheric emissions. Global Biogeochemical Cycles, 13(4), 933-950.

Byun D.W. and J.K.S. Ching, Eds. (1999) Science Algorithms of the EPA Models-3 Community Multiscale Air Quality (CMAQ) Modeling System. EPA/600/R-99/030, NERL, Research Triangle Park, NC, USA.

Byun D.W., S.T. Kim, F.Y. Cheng, S.B. Kim, A. Cuclis, and N.K. Moon (2003) Information infrastructure for air quality modeling and analysis: Application to the Houson-Galveston Ozone non-attainment area. J. Environ. Informa., 2(2), 38-57.

Byun D.W. and K.L. Schere (2006) Review of the governing equations, computational algorithms, and other components of the models-3 Community Multiscale Air Quality (CMAQ) modeling system. Applied Mechanics Reviews, 59(2), 51-77.

Damoah R., N. Spichtinger, C. Forster, P. James, I. Mattis, U. Wandinger, S. Beirle, T. Wagner, and A. Stohl (2004) Around the world in 17 days-hemispheric-scale transport of forest fire smoke from Russia in May 2003. Atmos. Chem. Phys., 4, 1311-1321.

Grell G.A., J. Dudhia, and D.R. Stauffer (1994) A description of the fifth-generation Penn State/NCAR mesoscale model (MM5), NCAR Technical Note, NCAR/TN-397+IA, 114.

In H.-J. and S.-U. Park (2002) A simulation of long-range transport of Yellow Sand observed in April 1998 in Korea. Atmos. Environ., 36(26), 4173-4187.

In H.-J., D.W. Byun, R.J. Park, N.-K. Moon, S. Kim, and S. Zhong (2007) Impact of transboundary transport of carbonaceous aerosols on the regional air quality in the United States: A case study of the South American wildland fire of May 1998. J. Geophys. Res., 112, D07201, doi:10.1029/2006JD007544.

Jaffe D., I. Bertschi, L. Jaegle, P. Novelli, J.S. Reid, H. Tanimoto, R. Vingarzan, and D.L. Westphal (2004) Long-range transport of Siberian biomass burning emissions and impact on surface ozone in western North America. Geophys. Res. Lett., 31, L16106, doi: 10.1029/2004GL020093.

Kaufman Y.J., C.O. Justice, L.P. Flynn, J.D. Kendall, E.M. Prins, L. Giglio, D.E. Ward, P. Menzel, and A.W. Setzer (1998) Potential global fire monitoring from EOS-MODIS. J. Geophys. Res., 103(D24), 32215-32238.

Lee K.H., J.E. Kim, Y.J. Kim, J.H. Kim, and W. von Hoyningen-Huene (2005) Impact of the smoke aerosols from Russian forest fires on the atmospheric environment over Korea during May 2003. Atmos. Environ., 39(1), 85-99.

Levine J.S., W.R. Cofer, D.R. Cahoon, and E.L. Winstead (1995) Biomass burning: A driver for global change. Environ. Sci. and Tech., 29(3), 120A-125A.

Malm W.C., J.F. Sisler, D. Huffmans, R.A. Eldred, and T.A. Cahill (1994) Spatial and seasonal trends in particle concentration and optical extinction in the United States. J. Geophys. Res., 99(D1), 1347-1370.

Malm W.C., D.E. Day, S.M. Kreidenweis, J.L. Collett, Jr., C.M. Carrico, G. McMeeking, and T. Lee (2005) Hygroscopic growth properties of an organic-laden aerosol. Atmos. Environ., 39(27), 4969-4982.

Pitchford M.L. and W.C. Malm (1994) Development and applications of a standard visual index. Atmos. Environ., 28(5), 1049-1054.

Seiler W. and P.J. Crutzen (1980) Estimates of gross and net fluxed of carbon between the biosphere and the atmosphere from biomass burning. Climate Change, 2(3), 207-247.

Streets D.G., T.C. Bond, G.R. Carmichael, S.D. Fernandes, Q. Fu, D. He, Z. Klimont, S.M. Nelson, N.Y. Tsai, M.Q. Wang, J.-H. Woo, and K.F. Yarber (2003) An inventory of gaseous and primary aerosol emissions in Asia in the year 2000. J. Geophys. Res., 108(D21), 8809, doi:10.1029/2002JD003093.

(Received 9 March 2009, accepted 27 May 2009)